Published in final edited form as:
Anal Chem. 2011 March 15; 83(6): 2279–2285. doi:10.1021/ac103161b.

Simultaneous Detection of Single Molecules and Singulated Ensembles of Molecules Enables Immunoassays with Broad Dynamic Range

David M. Rissin, **David R. Fournier**, **Tomasz Piech**, **Cheuk W. Kan**, **Todd G. Campbell**, **Linan Song**, **Lei Chang**, **Andrew J. Rivnak**, **Purvish P. Patel**, **Gail K. Provuncher**, **Evan P. Ferrell**, **Stuart C. Howes**[†], **Brian A. Pink**, **Kaitlin A. Minnehan**, **David H. Wilson**, and **David C. Duffy**[*]
Quanterix Corporation, One Kendall Square, Suite B14201, Cambridge, MA 02139, USA

Abstract

We report a method for combining the detection of single molecules (digital) and an ensemble of molecules (analog) that is capable of detecting enzyme label from 10^{-19} M to 10^{-13} M, for use in high sensitivity enzyme-linked immunosorbent assays (ELISA). The approach works by capturing proteins on microscopic beads, labeling the proteins with enzymes using a conventional multi-step immunosandwich approach, isolating the beads in an array of 50-femtoliter wells (Single Molecule Array, SiMoA), and detecting bead-associated enzymatic activity using fluorescence imaging. At low concentrations of proteins, when the ratio of enzyme labels to beads is less than ~1.2, beads carry either zero or low numbers of enzymes, and protein concentration is quantified by counting the presence of "on" or "off" beads (digital regime)[1]. At higher protein concentrations, each bead typically carries multiple enzyme labels, and the average number of enzyme labels present on each bead is quantified from a measure of the average fluorescence intensity (analog regime). Both the digital and analog concentration ranges are quantified by a common unit, namely, average number of enzyme labels per bead (AEB). By combining digital and analog detection of singulated beads, a linear dynamic range of over 6 orders of magnitude to enzyme label was achieved. Using this approach, an immunoassay for prostate specific antigen (PSA) was developed. The combined digital and analog PSA assay provided linear response over approximately four logs of concentration ([PSA] from 8 fg/mL – 100 pg/mL or 250 aM – 3.3 pM). This approach extends the dynamic range of ELISA from picomolar levels down to sub-femtomolar levels in a single measurement.

Introduction

The enzyme-linked immunosorbent assay (ELISA)[2-4] has been the cornerstone of sensitive detection of proteins for almost 40 years. ELISA is based on the ensemble detection of many enzyme-labeled proteins in μL to mL volumes, and has typically been limited to detecting picomolar (pM) concentrations of proteins. We recently reported a method called digital ELISA[1] based on single molecule arrays (SiMoA)[5-8] that allows the detection of single enzyme-labeled immunocomplexes by confining them to fL volumes. This approach resulted in a dramatic improvement in immunoassay sensitivity using ELISA reagents, such that sub-femtomolar concentrations of proteins could be detected in serum[1]. In this paper,

[*]Author to whom correspondence should be addressed: dduffy@quanterix.com.
[†]Current Address: Biophysics Graduate Group, 299 Life Science Addition, MC 3200, University of California, Berkeley, CA 94720-3200

Supporting Information Available: This material is available free of charge via the Internet at http://pubs.acs.org.

we extend this method to determining wider ranges of concentration by combining single molecule and ensemble detection in one straightforward measurement. This approach has allowed us to measure prostate specific antigen (PSA) in serum over a broad concentration range relevant to a particular clinical application. This paper makes use of several acronyms and symbols; for convenience, Table 1 provides a summary of their definitions. Many immunodiagnostic applications require both sensitive protein detection and broad analytical ranges (> 3 logs in concentration) in order to detect the target protein in the majority of samples. One such example is the detection of PSA in subjects who have undergone radical prostatectomy (RP). We have shown that digital ELISA can measure PSA levels in all men classified as undetectable by conventional immunoassay technology, the lowest being a patient with a PSA level of 14 fg/mL.[1] Measurement of very low levels of PSA may lead to expedited detection of a cancer recurrence event when compared to a conventional ELISA measurement[9]. PSA levels in some RP patients, however, are known to reach 100 pg/mL shortly after surgery[9], so PSA levels can span four logs of concentration in one group of patients. In another example, sensitive measurements of low levels of the serum biomarkers alpha fetoprotein and β-human chorionic gonadotropin[10] could be used to monitor patients for recurrence of testicular cancer after retroperitoneal lymph node dissection. Pre-surgery levels of alpha fetoprotein and β-human chorionic gonadotropin are known to span >3-logs of concentration in these patients,[10] with levels dropping below the detection limit of current assays post-surgery[11], suggesting clinical utility for highly sensitive assays with wide dynamic ranges. In addition, the hormone estradiol is routinely measured to assess the reproductive function in pre-menopausal women where concentration ranges in serum are greater than five logs[12]. Immunoassays for estradiol have also been used to identify pre- and post-menopausal women at risk for breast cancer, and to monitor for breast cancer recurrence where the absolute concentration of circulating estradiol is much lower[13,14]. Again, a highly sensitive immunoassay with a broad dynamic range is needed to fulfill the clinical need.

New ultra-sensitive immunoassays[1,15-17] are needed because the concentration of many biomarkers extend below the working range of currently used clinical assays, and its believed that most serum proteins are, in fact, currently undetectable[18]. Ultra-sensitive techniques are often capable of measuring low concentrations of a protein in a sample, but are not able to measure the high end of the concentration range without sample dilution and re-testing. It is often not possible, therefore, to measure the broad range of concentrations encountered in clinical samples in a single assay using ultra-sensitive methods. While diluting sample circumvents the insufficient working range of ultra-sensitive assays, in a clinical setting it is preferable to measure all samples in a single pass. By successfully quantitating the concentration of protein in the vast majority of samples in a single test, assay throughput and result turnaround time to the clinician will be improved.

Here, we present a technique for extending digital measurement of enzyme labels using SiMoA into the analog regime, enabling linear detection of enzyme label across six logs of concentration. With the goal of extending the working range of immunoassays, we applied this technique to digital ELISA for PSA. The working range of the combined digital and analog PSA assay was > 4 logs, detecting PSA in serum from 0.008 pg/mL to 100 pg/mL.

Experimental Section

Materials and Methods

The materials and procedures used for forming enzyme-labeled complexes on beads in the enzyme label and PSA assays, preparing femtoliter-volume well arrays, and loading beads into these arrays have been described elsewhere[1] and are provided in the Supporting Experimental Section.

Imaging and analysis of beads and enzyme-associated beads in femtoliter-volume well arrays

A microscope-based imaging system, containing a mercury light source, filter cubes, objectives, and a CCD camera was used to image enzyme-associated beads in well arrays formed at the end of fiber bundles[19,8]. Strips of eight fiber bundles arrays were assembled by gluing the bundles into custom-made glass holders. A strip was clamped on the microscope stage using a custom fixture. A droplet of substrate to β-galactosidase (RGP) was placed on a silicone gasket material and placed in contact with the well arrays. A precision mechanical platform moved the silicone gasket into contact with the end of the fiber bundle, creating an array of isolated femtoliter-volume reaction vessels containing RGP. Fluorescence images were acquired (577 nm excitation; 620 nm emission) with an exposure time of 1011 ms to detect enzymatic activity in the wells. Five fluorescence images (at 30-s intervals) were taken for each femtoliter-volume well array. After acquiring the fluorescence images, the arrays were illuminated with white light and imaged on the CCD camera. The white light and fluorescence images were analyzed using customized software to determine the presence of beads and enzymatic activity, respectively. First, the white light image was analyzed to determine which wells contained a bead. Due to scattering of light by the beads, those wells that contained a bead appeared brighter in the image than wells without beads. Second, regardless of signal levels, all fluorescence images were analyzed the same way. The fluorescence intensities of each well in each array of all five fluorescent images were first determined. The digital signal ("on" or "off") of each well containing a bead was assigned by determining whether or not the fluorescence intensity increased in each successive image, and by at least 20% over four images. Wells containing a bead that met these criteria were assigned as "on" or active; those that did not meet these criteria were assigned as "off". The digital signal, i.e., the fraction of "on" beads for each array (f_{on}), was then determined. The analog signal of each "on" bead was determined from the difference in its fluorescence intensity between the second and first fluorescence images ($I_{bead,F2}-I_{bead,F1}$). The analog signal of the array ($\bar{I}_{bead}$) was the average of $I_{bead,F2}-I_{bead,F1}$ over all "on" beads.

Results and Discussion

Singulated Bead ELISA Format

In the first step of the singulated bead ELISA, microscopic beads coated in antibodies capture the target protein from serum, plasma, or another complex sample, followed by labeling the bound proteins with enzyme reporter molecules. Enzyme labeling of the proteins is achieved by the formation of an immunocomplex in two steps, using a biotinylated detection antibody and a streptavidin-enzyme conjugate. The capture beads are then loaded into an array of femtoliter-sized microwells and the loaded array is sealed against a silicone gasket in the presence of a droplet of fluorogenic enzyme substrate, isolating each bead in a femtoliter reaction chamber. Beads associated with bound enzyme label or labels generate a locally high concentration of fluorescent product in the 50-fL reaction chambers. By using standard fluorescence imaging, it is possible to image tens of thousands of enzyme-associated beads simultaneously (Figure S-1). Depending on the fraction of beads that have one or more enzymes associated with them, the assay signal is determined by either digital or analog analysis methods to quantify the number of enzyme labels per bead detected (Figure 1). Figure S-1 contains examples of fluorescence images that are represented schematically in Figure 1. At low ratios of enzyme labels to beads, where there are a significant number of beads that are associated with no enzyme ("off" beads), the number of active, enzyme-associated (or "on") beads relative to the total number of beads detected are used to determine an average enzyme per bead (AEB) via Poisson statistics. As concentration is determined from counting "on" beads and is independent of

the fluorescence intensity generated in the well, we refer to this approach as 'digital'. At higher ratios of enzyme labels to beads, when most beads have one or more enzyme labels bound, the counting approach no longer works. In this situation, AEB (and, therefore, protein concentration) is determined from the average fluorescence intensity of wells containing a bead in the array ($\bar{I}_{bead}$); we refer to this approach as 'analog'. Currently, the analog approach is used to analyze images with >70% active beads. To convert $\bar{I}_{bead}$ to AEB in the analog regime, we make use of the digital measurements. First, images with <10% active beads are used to determine the average analog intensity of a single enzyme molecule ($\bar{I}_{single}$). The ratio of $\bar{I}_{bead}$ to $\bar{I}_{single}$ over all beads provides the analog AEB. The digital and analog analytical regimes are described in detail below.

Digital Determination of Protein Concentration

To determine protein concentration in samples, known standards are spiked into bovine serum or plasma, and SiMoA is used to generate a calibration curve of AEB versus concentration. SiMoA is then used to determine AEB for unknown samples that are compared to the calibration curve to determine concentration. At low ratios of enzymes to beads, when there are a statistically significant number of beads with no enzymes, by measuring the fraction of active beads in a population it is possible to determine the bulk analyte concentration because the binding probability of a population of analyte molecules to a population of beads is defined by the Poisson distribution. At very low ratios of labeled analyte to beads (less than about 0.1 enzyme labels per bead), most beads have either zero or one labeled analyte molecules and the percentage of active beads increases approximately linearly with increasing analyte concentration. As the fraction of active beads becomes larger (> 0.1), Poisson statistics show that there are a significant number of beads with multiple enzymes. If the fraction of active beads is plotted against concentration, linearity is lost at high target concentrations because active beads that have multiple enzyme molecules bound contribute the same 'digital' signal as an active bead that has one enzyme bound (Figure S-2). To quantitate the number of detected enzymes and to maintain linearity in the sub-populations of beads with multiple enzymes, we use Poisson statistics to convert the fraction of active beads to AEB.

The Poisson distribution (eq.1) describes the likelihood of a number of events occurring if the average number of events is known. If the expected average number of occurrences is μ, then the probability that there are exactly ν occurrences (ν being a non-negative integer, ν = 0, 1, 2, 3,…) is equal to:

$$P_{\mu}(\nu)=e^{-\mu}\left(\frac{\mu^{\nu}}{\nu!}\right) \quad (1)$$

In digital ELISA, μ is equal to the ratio of bound labeled proteins to the number of beads, and ν is the number of enzyme-labeled proteins carried by each sub-population of beads (i.e., 0, 1, 2, 3, etc.). The aim of the SiMoA experiment is to determine μ—which by definition is equal to AEB—and use it as the quantitative parameter to determine protein concentration. In the digital mode of analysis where beads are identified as being either "on" or "off", then ν = 1, 2, 3 are indistinguishable and characterized as "on" beads. A bead associated with one enzyme is indistinguishable from a bead associated with two enzymes due to the static heterogeneity of enzyme activity, where populations of individual enzyme molecules have been shown to have up to a seven-fold distribution in enzymatic activity[6,20-22]. Due to this broad distribution, only occurrences of ν = 0 can by determined definitively as the fraction of "off" beads ($P_{\mu}(0)$). Using eq.1 to determine $P_{\mu}(0)$, and the fact that the fraction of "off" beads is equal to one minus the fraction of "on" beads, it is

possible to determine $AEB_{digital}$ (the digitally-determined AEB) from f_{on} (the fraction of "on" beads or % active) (eq.2):

$$\mu = AEB_{digital} = -\ln[1 - f_{on}] \tag{2}$$

Figure S-2 demonstrates the effectiveness of the Poisson distribution analysis in the digital range of a calibration curve using an assay for streptavidin-β-galactosidase (SβG) that creates beads with well-defined enzyme/bead ratios[1]. In brief, beads were functionalized with a biotinylated capture molecule, and these beads were used to capture various concentrations of the SβG enzyme conjugate that we use as a label in digital ELISA. The beads were loaded into the femtoliter arrays and, after sealing a solution of RGP into the wells of the array, fluorescence was generated from bound enzymes accumulated in the reaction chambers for 2.5 min, with fluorescent images acquired every 30 s. A white light image of the array was acquired at the end of the experiment. These images were analyzed to identify wells that contained beads (from the white light image) and determine which of those beads had associated bound enzyme molecules (from time-lapsed fluorescent images), as described previously[1]. Figure S-2 shows that $AEB_{digital}$ determined from eq.2 maintained a linear response up to 50% active, despite non-linear variation in f_{on}.

Analog Determination of Protein Concentration

While quantification of concentration using counting and Poisson statistics works well below 70% active beads, as the fraction of active beads exceeds about 70%, the change in AEB with concentration is reduced leading to greater imprecision of concentration determination (Figure 2A). The counting approach ultimately breaks down when every bead has at least one bound enzyme.

We extend the dynamic range of the SiMoA assay beyond the digital regime by measuring the average fluorescence intensity of wells that contain beads to determine the number of enzymes associated with each bead detected. For this analysis, AEB can be determined from the average fluorescence intensity value of the active beads ($\bar{I}_{bead}$) and the average fluorescence intensity generated by a *single enzyme* ($\bar{I}_{single}$). The AEB of an array in the analog range (AEB_{analog}) is defined by eq. 3:

$$AEB_{analog} = \frac{f_{on} \times \bar{I}_{bead}}{\bar{I}_{single}} \tag{3}$$

To determine $\bar{I}_{single}$, we equate the digital (eq.2) and analog (eq.3) AEB terms at fractions of active beads where single enzymes dominate and substrate depletion is negligible (eq.4); we chose arrays with fractions of "on" beads <0.1 that meet these criteria:

$$\bar{I}_{single} = \frac{f_{on} \times \bar{I}_{bead}}{-\ln[1 - f_{on}]}, \text{ in arrays where } f_{on} < 0.1 \tag{4}$$

AEB can then plotted for both the digital ($AEB_{digital}$ (eq.2)) and analog (AEB_{analog} (eq.3)) ranges, and the two curves are seamlessly meshed into one calibration curve.

In order to combine digital and analog data, each experiment ideally requires arrays where the fraction of active beads is less than 10% (eq.4). This requirement is achieved using the calibration data points that cover this range, or specific control samples known to have this digital signal. With two or three concentrations in a calibration curve with $f_{on} < 0.1$, the kinetic activities of thousands of individual enzyme molecules are averaged to determine $\bar{I}_{single}$. Because the activities of thousands of molecules are averaged, the intrinsic variation associated with single enzyme molecule velocities described above does not add significant variation to the $\bar{I}_{single}$ measurement. The width parameter ($\sigma_{\bar{I}_{slngle}}$) of the mean single enzyme intensity ($\bar{I}_{single}$) as a function of *N* measurements[23] is given by $\sigma_{I_{single}} / \sqrt{N}$, where $\sigma_{I_{single}}$ is the width parameter of single enzyme molecule intensities. With a 30% CV in single enzyme molecule intensities[6], the variation added to the CV of the calculated mean value $\bar{I}_{single}$ is 1% when averaging over 1000 single molecule measurements.

There is a significant range of fraction of active beads (10–99.98%) where theoretically digital counting and analog intensities could both be used to determine AEB. Below 10%, the contribution of beads associated with multiple enzymes is small and $\bar{I}_{bead}$ does not vary above measurement noise with % active, so the analog approach does not work. As f_{on} approaches 100%, counting cannot be used to digitally determine AEB. Between these two extremes, imprecision considerations (manifested by the coefficient of variation (% CV) of AEB) determine the threshold of the fraction of active beads below which $AEB_{digital}$ (eq.2) is used and above which AEB_{analog} (eq.3) is used. The choice of this threshold is illustrated by plotting the imprecision in AEB arising from the variation in digital and analog signals from 10–100% active beads (Figure 2C). Close to 10% active beads, changes in $\bar{I}_{bead}$ above single molecule values are small as AEB increases, leading to high imprecision in AEB. As the % active goes above 70% and the Poisson distribution curves deviates from linearity, the change in $AEB_{digital}$ with % active decreases leading to greater imprecision in the $AEB_{digital}$ determined. The balance of imprecision profiles in this overlap zone (Figure 2C) led us to choose the ‘digital-to-analog’ threshold as 70% active (around AEB = 1.2).

Combined digital and analog enzyme label detection

The SβG binding assay described in the Supporting Experimental Section and elsewhere[1] was used to demonstrate the dynamic range to enzyme label that can be achieved by combining digital and analog determination of AEB. Figure 3 shows AEB determined from SiMoA images of populations of biotin-presenting beads that had been incubated with concentrations of SβG ranging from zeptomolar to picomolar. For images with % active beads < 70%, $AEB_{digital}$ was determined using eq.2. All the arrays with <10% active beads were used to determine $\bar{I}_{single}$, a total of 7566 beads; $\bar{I}_{single}$ was equal to 298 au. The average fluorescence intensities of beads in images with over 70% active were determined, and AEB_{analog} values were calculated using eq. 3. Because the 0 M SβG concentration yielded no active beads, the lower limit of detection in this experiment could not be calculated using the background plus 3 s.d. method. Using our previously established LOD of 220 zM[1], and the highest concentration detected in the linear range of this curve, 316 fM, we determined a 6.2-log linear dynamic range for detecting enzyme label. The linear digital dynamic range was 4.7 logs; the analog linear dynamic range was 1.5 logs.

The dynamic range of the analog SiMoA measurement is affected by substrate depletion, timing of sealing and imaging by the system, and dynamic range of the camera. These issues are discussed in detail in the Supporting Text.

Combined digital and analog ELISA for measuring PSA in serum

We next sought to implement the combined digital and analog approach to develop a SiMoA ELISA for PSA with a wide dynamic range. Clinically, PSA is used to screen for prostate

cancer and to monitor for biochemical recurrence of the disease in patients who have undergone surgery to remove the cancer. The PSA levels in the serum of patients who have undergone radical prostatectomy (RP) are known to range from 0.014 pg/mL[1] to over 100 pg/mL[9]. To successfully measure the PSA levels in the majority of patients in a single test requires an assay with 4 logs of dynamic range. A SiMoA ELISA for PSA was developed and run as described in the Supporting Experimental Section. Figure 4 shows that by combining digital and analog analyses, the working range of the SiMoA PSA assay was from 0.008 pg/mL to 100 pg/mL, enabling precise quantification of PSA levels in the vast majority of RP patient samples in one pass.

We used this assay to measure the concentration of PSA in the sera of 17 prostate cancer patients collected at 2 to 46 weeks (mean = 13.8 weeks) after radical prostatectomy surgery. These samples were collected closer to surgery than our previous study[1] that—in order to push the lower limits of detection of digital ELISA—tested samples collected an average of 8 years post-surgery of patients whose cancer did not recur. Here, in order to evaluate the dynamic range of the assay across the intended clinical range, samples collected closer to surgery were tested to capture patients with higher PSA whose cancer could recur. PSA was, however, undetectable in all of these samples using a leading PSA diagnostic test (Siemens). Serum samples were diluted 1:4 in buffer and AEB was measured using SiMoA. The concentration of PSA for each sample was determined by reading the AEB off a simultaneously acquired calibration curve similar to Figure 4. Table 2 summarizes the AEB and PSA concentrations determined from these samples, along with the imprecision for signal and concentration given by % CV. PSA was quantified in all of the samples in one experiment. The average PSA concentration in these samples was 33 pg/mL, with a high of 136 pg/mL and a low of 0.4 pg/mL. When combined with our previous measurements of PSA in RP patients[1], SiMoA has detected concentrations of PSA in clinical samples from 0.46 fM (0.014 pg/mL) to 4.5 pM (136 pg/mL), demonstrating the importance of an assay with good dynamic range. The PSA levels in Table 2 are significantly higher than from the set of samples that we previously tested[1] that were collected from known, non-recurring patients, typically several years post-surgery. Presumably, the levels detected in this study are more indicative of patients soon after surgery, and will contain individuals whose cancer might recur.

Conclusions

The transition from extremely sensitive digital detection of single molecules to analog detection of ensembles of molecules was achieved with two enhancements to the SiMoA approach. First, a Poisson distribution analysis was applied to account for both single and multiple enzymes per bead from 0–70% active to determine the digital AEB value. Second, the average analog intensities of beads in images at over 70% active beads were converted to AEB using the average intensity for a single enzyme. These two analytical approaches permit linear measurement of AEB from 0.00005 to ~15. For PSA, combining the analog and digital analyses extended the working range to 4.1 logs of concentration from the original digital working range of 2.5 logs.

We are currently working on extending the working range of SiMoA an additional 1–2 orders of magnitude by improving the speed of the imaging system and minimizing the impact of substrate depletion. By further expanding the range of our assays, we hope to successfully measure all samples in a single assay cycle to improve assay throughput and reduce the cost of immunoassays.

Supplementary Material

Refer to Web version on PubMed Central for supplementary material.

Acknowledgments

The authors thank Dr. David Hanlon for helpful discussions. The project described was supported in part by Award Number R43CA133987 from the National Cancer Institute.

References

1. Rissin DM, Kan CW, Campbell TG, Howes SC, Fournier DR, Song L, Piech T, Patel PP, Chang L, Rivnak AJ, Ferrell EP, Randall JD, Provuncher GK, Walt DR, Duffy DC. Nat Biotech 2010;28:595–599.
2. Gosling JP. Clin Chem 1990;36:1408–1427. [PubMed: 2201458]
3. Wild, D. The Immunoassay Handbook, 3rd Edition. Third Edition. Elsevier; 2005.
4. Zhang HQ, Zhao Q, Li XF, Le XC. Analyst 2007;132:724–737. [PubMed: 17646870]
5. Gorris HH, Rissin DM, Walt DR. Proc Nat Acad Sci 2007;104:17680–17685. [PubMed: 17965235]
6. Rissin DM, Gorris HH, Walt DR. J Am Chem Soc 2008;130:5349–5353. [PubMed: 18318491]
7. Rissin DM, Walt DR. J Am Chem Soc 2006;128:6286–6287. [PubMed: 16683771]
8. Rissin DM, Walt DR. Nano Lett 2006;6:520–523. [PubMed: 16522055]
9. Eisenberg, ML.; Davies, BJ.; Cooperberg, MR.; Cowan, JE.; Carroll, PR. Prognostic Implications of an Undetectable Ultrasensitive Prostate-Specific Antigen Level after Radical Prostatectomy. Vol. 57. Elsevier; Kidlington, ROYAUME-UNI: 2010.
10. Spiess PE, Brown GA, Liu P, Tannir NM, Tu SM, Evans JG, Czerniak B, Kamat AM, Pisters LL. Cancer 2006;107:1483–1490. [PubMed: 16944541]
11. Bartlett N, Freiha F, Torti F. Hematol Oncol Clin North Am 1991;5:1245. [PubMed: 1723408]
12. Burger HG, Dudley EC, Hopper JL, Groome N, Guthrie JR, Green A, Dennerstein L. J Clin Endocrinol Metab 1999;84:4025–4030. [PubMed: 10566644]
13. Group, E. H. a. B. C. C. Cancer Epidemiology Biomarkers & Prevention 2003;12:1457–1461.
14. Eliassen AH, Missmer SA, Tworoger SS, Spiegelman D, Barbieri RL, Dowsett M, Hankinson SE. J Natl Cancer Inst 2006;98:1406–1415. [PubMed: 17018787]
15. Armani AM, Kulkarni RP, Fraser SE, Flagan RC, Vahala KJ. Science 2007;317:783–787. [PubMed: 17615303]
16. Bao YP, Wei TF, Lefebvre PA, He HAL, Kunkel GT, Muller UR. Anal Chem 2006;78:2055–2059. [PubMed: 16536446]
17. Todd J, Freese B, Lu A, Held D, Morey J, Livingston R, Goix P. Clin Chem 2007;53:1990–1995. [PubMed: 17890441]
18. Anderson NL, Polanski M, Pieper R, Gatlin T, Tirumalai RS, Conrads TP, Veenstra TD, Adkins JN, Pounds JG, Fagan R, Lobley A. Molecular & Cellular Proteomics 2004;3:311–326. [PubMed: 14718574]
19. Pantano P, Walt DR. Chem Mater 1996;8:2832–2835.
20. Craig DB, Arriaga EA, Wong JCY, Lu H, Dovichi NJ. J Am Chem Soc 1996;118:5245–5253.
21. Craig DB, Dovichi NJ. Can J Chem 1998;76:4.
22. Xue Q, Yeung ES. Nature 1995;373:681–683. [PubMed: 7854448]
23. Taylor, JR. An Introduction to Error Analysis : The Study of Uncertainties in Physical Measurements. Sausalito, EUA: University Science Books; 1997.

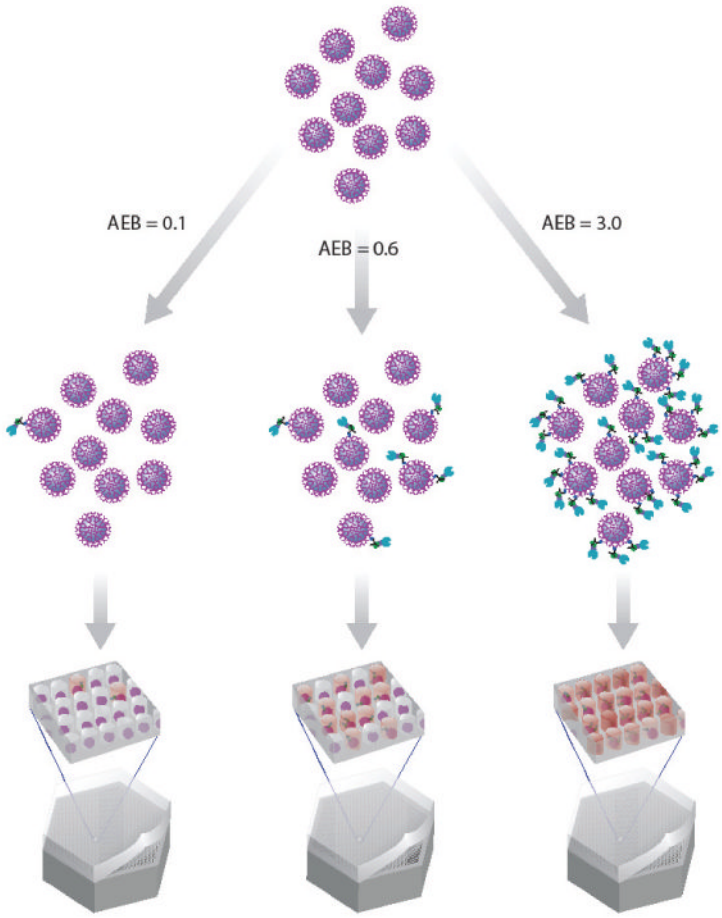

Figure 1.

The signal output of SiMoA at different regimes of enzyme/bead ratios. (Left) At AEB = 0.1, active beads are statistically associated predominantly with single enzymes, and the SiMoA readout is “single molecule”. (Center) At AEB = 0.6, a significant number of active beads have multiple enzymes bound. The images are still analyzed by counting “on” wells so quantitation is digital. Multiple enzymes per bead are accounted for in data analysis using the Poisson distribution. (Right) At AEB = 3, every bead has at least one enzyme associated with it. In this case, the average number of enzymes per bead is quantitated by measurement of the average fluorescence intensity of the active beads and from knowledge of the average fluorescence intensity generated by a single enzyme.

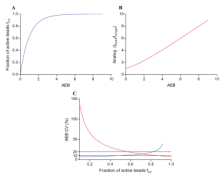

Figure 2.

(A) Plot of fraction of active beads against the effective concentration—given by AEB—determined from digital counting using the Poisson distribution (eq. 2). As concentration increases, the slope of % active gets shallower and signal imprecision leads to greater imprecision in concentration determined. (B) Plot of analog intensity (I_{bead}/I_{single}) as a function of effective concentration, AEB (eq.3). At low concentrations, variation in intensity measurements makes it impractical to detect small increases in multiple enzymes and CVs of extrapolated AEB are high. (C) Plots of imprecision in AEB (% CV) as a function of f_{on} from digital (blue line) and analog (red line) analyses assuming a fixed signal CV of 7.1% for both methods. This signal CV was determined empirically by fitting AEB imprecision data from the PSA digital ELISA collected over six days.

A

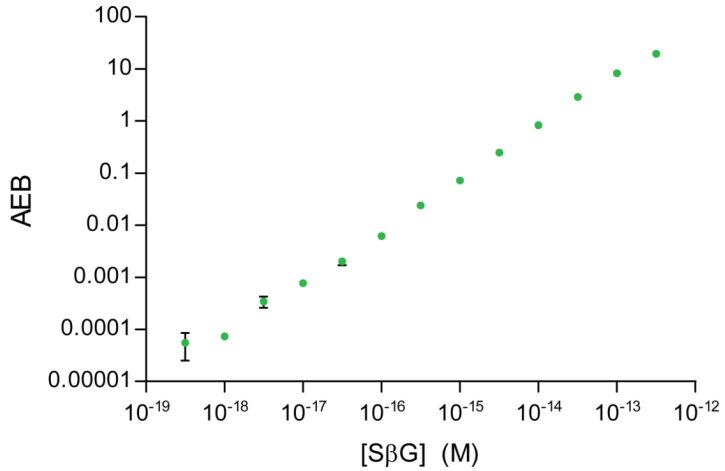

B

[SβG] (M)	f_{on} (% active)	AEB $AEB_{digital}$ or AEB_{analog}	% CV AEB
0	0	0	0%
3.16×10^{-19}	0.006	5.5×10^{-5}	54%
1.00×10^{-18}	0.007	7.3×10^{-5}	ND
3.16×10^{-18}	0.03	3.4×10^{-4}	25%
1.00×10^{-17}	0.08	7.7×10^{-4}	11%
3.16×10^{-17}	0.20	2.0×10^{-3}	16%
1.00×10^{-16}	0.62	6.2×10^{-3}	7%
3.16×10^{-16}	2.36	2.39×10^{-2}	5%
1.00×10^{-15}	6.99	7.25×10^{-2}	5%
3.16×10^{-15}	21.89	0.2470	<1%
1.00×10^{-14}	56.16	0.8286	11%
3.16×10^{-14}	96.27	2.902	4%
1.00×10^{-13}	99.06	8.264	12%
3.16×10^{-13}	99.12	19.55	14%

Figure 3.

Broad dynamic range to enzyme label was achieved by combining digital and analog measurements in SiMoA. (**A**) Plot of AEB as a function of enzyme concentration. The error bars are standard deviations over three replicates. (**B**) % active and AEB values as a function of enzyme concentration. AEB was determined using eq. 2 for % active < 70%. AEB was determined using eq. 3 for % active > 70%. The threshold between analog and digital in this experiment was between 10 fM and 31.6 fM.

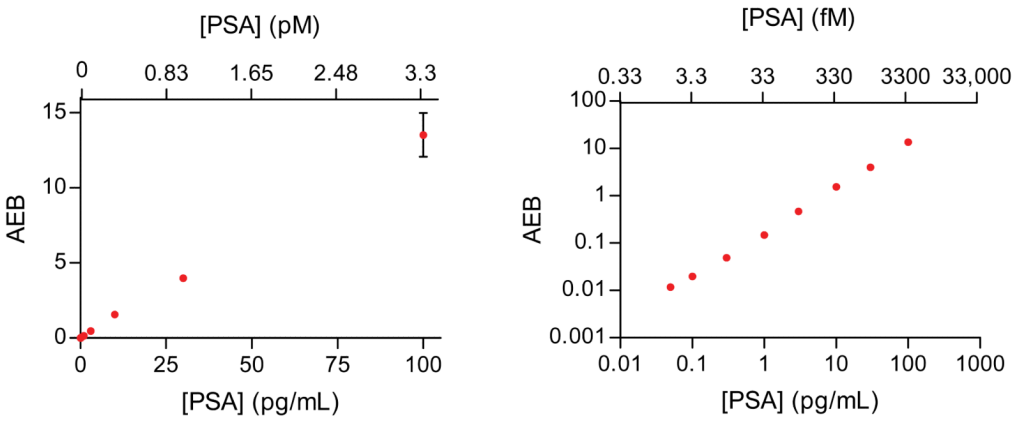

Figure 4.

The combined digital and analog SiMoA PSA assay with a 4-log working range and calculated LOD of 0.008 pg/mL. AEB is plotted as a function of PSA concentration in linear-linear space (left) and log-log space (right). Error bars are shown for all data points based on quadruplicate measurements.

Table 1

Definitions of some of the acronyms and symbols used in this paper.

Acronym	Definition
General	
ELISA	enzyme-linked immunosorbent assay
SiMoA	single molecule array
Analytical	
f_{on}	fraction of enzyme-associated (active) beads
AEB	average enzymes per bead
$AEB_{digital}$	AEB determined by counting active beads
AEB_{analog}	AEB determined from the average intensity of active beads
$\bar{I}_{bead}$	mean fluorescence intensity of active beads in an array
$\bar{I}_{single}$	mean fluorescence intensity generated by single enzymes on beads
Biological	
RGP	resorufin-β-D-galactopyranoside, a substrate of β-galactosidase
SβG	conjugate of streptavidin and β-galactosidase
PSA	prostate specific antigen
RP	radical prostatectomy

Table 2

Summary of AEB and [PSA] determined for 17 serum samples from post-RP patients. Standard deviations and CVs were determined over triplicate tests. Sample S644 had an AEB value beyond the range of the calibration curve but its concentration was determined by extrapolation.

Sample ID	Mean AEB	Std Dev AEB	AEB CV	[PSA] (pg/mL)	Std Dev [PSA]	[PSA] CV
S640	8.8	1.2	13%	41.0	7.5	18%
S641	0.87	0.08	10%	4.1	0.4	11%
S643	0.23	0.002	1%	1.1	0.01	1%
S644	15.2	1.0	6%	136	13	10%
S645	1.5	0.06	4%	6.1	0.2	4%
S647	11.0	0.1	1%	80.4	1.9	2%
S648	7.4	0.3	3%	32.3	1.6	5%
S649	1.5	0.2	11%	6.1	0.6	10%
S650	0.22	0.008	4%	1.2	0.03	2%
S651	0.50	0.02	5%	2.3	0.1	4%
S615	12.6	1.0	8%	70.7	8.6	12%
S653	1.3	0.2	18%	5.0	0.8	16%
S616	0.44	0.05	12%	1.7	0.2	13%
S618	13.6	0.7	5%	79.2	6.2	8%
S624	14.8	0.5	3%	88.9	4.1	5%
S627	0.098	0.003	3%	0.39	0.01	3%
S628	0.92	0.04	5%	3.7	0.15	4%